Inventory for Supplementary Information

Blm10 facilitates nuclear import of proteasome core particles

by **Marion H. Weberruss , Anca F. Savulescu , Julia Jando, Thomas Bissinger, Amnon Harel , Michael H. Glickman and Cordula Enenkel**

Figure S1 refers to Figure 1. (**A**) PSG and JUNQ are motile cytosolic clusters either formed upon proteasome inhibiton and cell cycle arrest (Kaganovich et al., 2008) or during quiescence (Laporte et al. 2008). (**B**) Blm10 is not required for the sequestration of RP base and lid complexes into PSG. (**C**) Ump1-associated precursor complexes are lacking in quiescent cells.

Figure S2 refers to Fig. 2. Assigment of CP and RP species.

Figure S3 refers to Fig. 3A. (**A**) Re-import studies of GFP-labelled RP lid in quiescent wild type and *blm10Δ* cells upon the resumption of growth. (**B**) Native PAGE analysis and GFP-imaging of lysates from wild type and *blm10Δ* cells expressing GFP-labelled β5 upon the resumption of cell growth.

Figure S4 refers to **Fig. 3B**. Re-import studies of GFP-labelled CP and Blm10 in quiescent *srp1-49* mutants upon the resumption of growth.

Figure S5 refers to **Fig. 4A**. Nuclear import of CP depends on RanGTP.

Figure S6. Bleomycin-hypersensitivity of quiescent *blm10Δ* cells.

1. Supplementary Methods for nuclear reconstitution reactions

Buffers

ELB – 10 mM Hepes pH7.4, 50 mM KCl, 2.5 mM $MgCl_2$, 1 mM DTT, 5μg/ml Cycloheximide, 5μg/ml Cytochalasin B, 10 μg/ml Aprotinin, 10 μg/ml Leupeptin.

ELBS – Egg Lysis Buffer buffer containing 250 mM Sucrose.

PBS pH7.4 – 137 mM NaCl, 10 mM Phosphate, 2 mM KCl.

Xenopus egg extracts and nuclear reconstitution

Preparation of demembranated sperm chromatin and *Xenopus* egg extracts as well as fractionation into cytosolic and membrane fractions were performed as previously described (Savulescu et al., 2011). Nuclei were reconstituted by mixing *Xenopus* egg membrane vesicles and cytosolic fractions at a 1:20 ratio, an ATP-regeneration system and sperm chromatin (ibid). Nuclear morphology was monitored by staining with Hoechst 33258 (Sigma-Aldrich) after 60 min of assembly. Nuclear pore complex formation was tested by staining with mAb414 (Covance). Once nuclear and NPC assembly had been confirmed, the reconstitution reactions were diluted by the addition of 3 volumes of 1xELBS and incubated for 15 min. Nuclear import capacity was tested by addition of tetramethyl rhodamine isothiocyanate-labeled (TRITC)-NLS-bovine serum albumin, a well established NLS-containing reporter protein of nuclear import (ibid). Once nuclear and NPC assembly had been confirmed, the reconstitution reactions were diluted by the addition of 3 volumes of 1xELBS and incubated for 15 min. For the reconstitution of Blm10-bound CP, ~ 0.2 μg Oregon Green-labeled yeast CP was mock-treated with PBS or pre-incubated with ~ 0.4 μg Blm10 in PBS for 30 min in the dark at

room temperature prior to their addition to assembled nuclei. The dilution factor of labeled yeast CP in relation to the nuclei was kept constant in all experiments. For quantification, 30 nuclei of 3 independent experiments were randomly chosen and individually scored as having either a nuclear rim or intranuclear staining. Statistics was performed using ImageJ and Excel software.

Reconstitution experiments with the calcium chelator BAPTA which does not allow the formation of functional nuclear pore complexes revealed that Oregon Green-labeled CP does not bind BAPTA-treated nuclei. This finding suggests that Oregon Green-labeled CP from yeast binds to nuclear pore complexes from *Xenopus* and may explain why some Oregon Green-labeled CP decorates the nuclear rim without Blm10 (see **Fig. 3B**).

Oregon Green labeling of purified yeast 20S CP

Purified CP from yeast were concentrated to ~0.75 mg/ml and labeled on exposed amine groups with Oregon Green 488 succinimidyl ester (Molecular Probes) for 1 h at 4°C. Unreacted dye was quenched with 0.1 M ethanolamine pH 8.0 for 2 h and removed by extensive dialysis followed by separation on a size exclusion Superose 6 gel filtration column (GE-healthcare). Oregon Green-labeled CP fractions eluted from the column were pooled and concentrated. Oregon Green-labeled CP was subjected to SDS-PAGE and visualized by Silver Stain. The fluorescent dye was conjugated to multiple subunits of the CP.

Consistent with previous results (Fehlker et al., 2003), Blm10-treated Oregon Green-labelled CP exhibited 30% peptide cleavage activity compared to mock-treated Oregon Green-labelled CP.

Immunofluorescence and Confocal microscopy

For direct visualization of Oregon Green-labeled CP, nuclei were fixed in 3% paraformaldehyde and stained with Hoechst 33258. Images were acquired on an Olympus BX61TRF epifluorescence microscope equipped with a DP70 digital camera or a Zeiss LSM 510 META confocal microscope. Figures were prepared using LSM software and Adobe Photoshop.

2. Supplementary Figure Legend

Figure S1. (**A**) PSG and JUNQ describe the same structure. According to previous studies by Frydman and her co-workers GFP-labelled Van-Hippel-Lindau-suppressor protein (GFP-VHL), an established reporter of misfolded proteins, is an indicator of JUNQ formation upon proteasome inhibition and cell cycle arrest (Kaganovich et al., 2008). To investigate whether GFP-VHL is stabilized in PSG, wild type cells expressing CFP-labelled CP and GFP-VHL were analyzed by direct fluorescence microscopy. During logarithmic phase, the staining of GFP-VHL was hardly detectable indicating that RP-CP assemblies achieve the degradation of GFP-VHL (Kaganovich et al., 2008). During quiescence, CFP-labelled CP and GFP-VHL co-localized in PSG suggesting that PSG and JUNQ describe the same subcellular structures (upper panel). Bar, 2 μm. Consistent with previous studies (Kaganovich et al., 2008; Laporte et al., 2008), GFP-VHL, CFP-labelled α4 (CP) and Blm10 are soluble in quiescent cells (lower panel). The VHL solubility and supernatant-pellet assays were performed according to (Kaganovich et al., 2008). T, total lysate; S, supernatant, and P, pellet after 16,000 x g centrifugation for 30 min at 4ºC. Protein molecular weight (kDa).

(**B**) GFP-labelled RP is monitored by direct fluorescence microscopy in yeast cells grown to logarithmic and stationary phase. Wild type and *blm10Δ* cells expressing either GFP-tagged Rpn1 or Rpn11 which are established reporter proteins of RP base and lid, respectively (Wendler et al., 2004), were monitored by direct fluorescence microscopy. Bar, 3 μm.

(**C**) Wild type and *blm10Δ* cells expressing GFPS-tagged Ump1, which is incorporated into precursor complexes (Fehlker et al., 2003), were monitored by direct fluorescence microscopy (GFP) and Nomarski optics (DIC). The insert shows 4,6-diamidino-2-phenylindole (DAPI)-staining of a yeast nucleus, as visualized by the UV filter and Nomarski optics. Bar, 3 μm.

Figure S2. Assignment of CP and RP configurations in wild type cells grown to logarithmic and stationary phase. Native PAGE gels were extracted from **Figs. 2A** and **2B**. The GFP moieties of the CP subunit β5 (Pre2) were visualized in gel by fluoroimaging. RP species were detected by immunoblotting against Rpt1, a RP base ATPase. CP and RP configurations were assigned according to previous studies (Lehmann et al, 2008; Li et al, 2007) (Kleijnen et al, 2007). To verify the assignment of RPn and RPnn the native PAGE of quiescent wild type cells was blotted and probed with anti-CP (β7, Pre4) antibodies. Consistent with the GFP image only a minor band corresponding to RP-CP assemblies was detected. Most CP migrate as free and Blm10-bound species. As loading control cell lysates were subjected to SDS-PAGE followed by immunoblotting against GFP-labelled β5.
RP-CP-RP, RP-CP and CP are also named 30S, 26S and 20S proteasomes, respectively, according to their Svedberg sedimentation coefficients (S).

Figure S3. (**A**) Re-import studies of GFP-labeled RP lid in quiescent wild type and *blm10Δ* cells upon the resumption of growth. Direct fluorescence microscopy of quiescent wild type and *blm10Δ* cells expressing GFP-labeled Rpn11 (left panels) and 5

min after the addition of fresh YPD (right panels). Quiescent wild type and *blm10Δ* cells expressing GFP-labeled Rpn1, a subunit of the RP base, displayed the same phenotype (not shown). Bar, 2μm.

(**B**) Native PAGE analysis and GFP-imaging of lysates from wild type (upper panel) and *blm10Δ* cells (lower panel) expressing GFP-labelled β5 upon the resumption of cell growth. According to **Fig. 3A** time point 0 indicates the addition of fresh YPD medium to stationary phase cells. At the times points indicated, cells were harvested and disintegrated in TB. Cell lysates were subjected to native PAGE followed by fluoroimaging. CP configurations were assigned as described in **Fig. S2**. In *blm10Δ* cells RP-CP assemblies increase, when CP precursor complexes are formed and imported into the nucleus again.

Figure S4. (**A**) Re-import studies of CP in quiescent *srp1-49* mutants expressing GFP-labelled β5 upon the resumption of growth. Cells were monitored by direct fluorescence microscopy before and 5 min after the addition of fresh YPD. Bar, 2 μm. (**B**) Re-import studies of Blm10 in quiescent *srp1-49* mutants expressing GFP-labelled Blm10 upon the resumption of growth. Cells were monitored by direct fluorescence microscopy before and 15 min after the addition of fresh YPD. Bar, 5 μm.

Figure S5. Nuclear import of CP depends on RanGTP. Nuclear targeting of Oregon-Green-labeled yeast 20S-CP in the presence or absence of RanQ69L in *in vitro* reconstituted *Xenopus* nuclei. Reconstituted nuclei were pre-incubated with buffer (mock) or 10 μM RanQ69L-GTP for 15 min before the addition of fluorescently tagged

20S-CP and TRITC-NLS-BSA, an established nuclear import substrate. Samples were fixed and analyzed by epifluorescence microscopy. TRITC-NLS-BSA accumulated in the nuclei, but not in the presence of RanQ69L. 20S-CP was targeted to the nuclear periphery as well as inside the nucleus. Its nuclear targeting was reduced in the presence of RanQ69L. Mean values of fluorescence intensities at the nuclear rim (white column) and inside the nucleus (grey column) were scored from 25-40 individual nuclei, that were either mock or treated with RanQ69L, and compiled in a histogram. Error bars represent the SE. Scale bars, 10 μm.

Figure S6. Quiescent *blm10Δ* cells are hypersensitive to phleomycin, a derivative of bleomycin. Wild type and *blm10Δ* cells either transformed with YCplac111 (YCp) or YCplac111-derived pTF167 expressing Blm10 behind the endogenous promoter (YCp *BLM10*) were grown to logarithmic and stationary phase, harvested and resuspended in H_2O. Aliquots of cells were treated with 1μg/ml phleomycin for 3h at 30 ºC, serially diluted and spotted on YPD. Plates were incubated for 2d at 30 ºC.

Background information. Initially, the bleomycin-sensitive phenotype of *blm10Δ* cells suggested that Blm10, formerly named Blm3, protects against bleomycin-induced DNA damage and oxidative stress (Febres et al, 2001). Later studies challenged these findings (Iwanczyk et al, 2006). Thus, we reinvestigated the cells sensitivity to phleomycin, a bleomycin derivative. Consistent with Iwanczyk et al. (2006) growing wild type and *blm10Δ* cells were not hypersensitive to phleomycin (**Fig. S6**; upper panel). However during quiescence, *blm10Δ* cells were more sensitive to phleomycin than wild type cells and unable to resume cell growth upon the exposure to phleomycin (lower panel).

Table I. Strains used in this work

Strain	Genotype	Fig
WCGa	*MAT***a** *his3-11,15 leu2-3,112 ura3-52 can GAL*	
blm10Δ	*MAT**a** his3-11,15 leu2-3,112 ura3-52 can GAL blm10Δ::HIS3*	
YMW1	*MAT***a** *his3-11,15 leu2-3,112 ura3-52 can GAL PRE2-GFPS-HIS3-URA3 HTA2-RFP-natMX*	1A
YMW3	*MAT**a** his3-11,15 leu2-3,112 ura3-52 can GAL blm10Δ::HIS3 PRE2-GFPS-HIS3-URA3 ± HTA2-RFP-natMX*	1B, 3A
YMW4	*MAT***a** *his3-11,15 leu2-3,112 ura3-52 can GAL Blm10-GFPHA-URA3-HIS3*	1C
YMW5	*MAT**a** his3-11,15 leu2-3,112 ura3-52 can GAL blm10Δ::HIS3 HTA2-RFP-natMX PRE6-GFPS-LEU2 [pTF155]*	1D
YMW6	*MAT***a** *his3-11,15 leu2-3,112 ura3-52 can GAL PRE2-GFPS-HIS3-URA3 ump1::YIplac128-UMP1-HA*	2AB, S2B
YMW7	*MAT**a** his3-11,15 leu2-3,112 ura3-52 can GAL blm10Δ::HIS3 PRE2-GFPS-HIS3-URA3 ump1::YIplac128-UMP1-HA*	2AB, S2B
YMW8	*MATα his3Δ200 leu2Δ1 trp1Δ63 ura3-52 gsp1-1 Blm10-GFPHA-URA3-HIS3*	4A
YMW9	*MATα ade2-101 his3Δ200 ura3-52 prp20-1 Blm10-GFPHA-URA3-HIS3*	4A
YMW10	*MAT***a** *his3-11,15 leu2-3,112 ura3-52 can GAL Blm10-GFPHA-URA3-HIS3 [pMK210-4]*	4A
YMW11	*MAT**a** his3-11,15 leu2-3,112 ura3-52 can GAL blm10Δ::HIS3 Pre6-ProA-LEU2 [pTF155]*	4B
YMW12	*MAT**a** his3-11,15 leu2-3,112 ura3-52 can GAL blm10Δ::HIS3 [pMW1]*	4C
YMW13	*MAT***a** *his3-11,15 leu2-3,112 ura3-52 can GAL [YCplac111]*	S6
YMW14	*MAT**a** his3-11,15 leu2-3,112 ura3-52 can GAL blm10Δ::HIS3 [YCplac111]*	S6
YMW15	*MAT**a** his3-11,15 leu2-3,112 ura3-52 can GAL blm10Δ::HIS3 [YCp BLM10 = pTF167]*	S6

YMW16	*MAT***a** *his3-11,15 leu2-3,112 ura3-52 can GAL PRE6-CFPHA-HIS3-URA3 [pESC-GFP-VHL-LEU2]*	S1A
YMW17	*MAT***a** *his3-11,15 leu2-3,112 ura3-52 can GAL RPN1-GFPS-HIS3-URA3*	S1B
YMW18	*MAT**a** his3-11,15 leu2-3,112 ura3-52 can GAL blm10Δ::HIS3 RPN1-GFPS-HIS3-URA3*	S1B
YMW19	*MAT***a** *his3-11,15 leu2-3,112 ura3-52 can GAL RPN11-GFPS-HIS3-URA3*	S1B, S2A
YMW20	*MAT**a** his3-11,15 leu2-3,112 ura3-52 can GAL blm10Δ::HIS3 RPN11-GFPS-HIS3-URA3*	S1B, S2A
YMW21	*MAT***a** *his3-11,15 leu2-3,112 ura3-52 can GAL UMP1-GFPS-HIS3-URA3*	S1C
YMW22	*MAT**a** his3-11,15 leu2-3,112 ura3-52 can GAL blm10Δ::HIS3 UMP1-GFPS-HIS3-URA3*	S1C
YMW23	*MAT***a** *ade2-1 trp1-Δ63 his3-11,15 leu2-3,112 ura3 –1 can1-100 srp1-49 PRE2-GFPS-HIS3-URA3*	S3A
YMW24	*MAT***a** *ade2-1 trp1-Δ63 his3-11,15 leu2-3,112 ura3 –1 can1-100 srp1-49 BLM10-GFPHA-URA3-HIS3*	S3B
YMW25	*MAT**a** his3-11,15 leu2-3,112 ura3-52 can GAL PRE6-ProA-URA3-HIS3 [pMK210-4]*	4F

References:

Derivatives of WCGa and *blm10Δ* (Fehlker et al., 2003)

gsp1-1 (Wong et al. 1997)

prp20-1 (Aebi et al., 1990)

srp1-49 (Yano et al. 1992)

Table II. Plasmids used in this work

Plasmid	Genotype	Fig
pTF155	YEp [GAL-His12-Blm10] URA3	1D, S4C
pMK210-4	YEp351[GAL-FLAG-GSP1-G21V-LEU2]	4AE
GST	pGEX-4T-3	4CDEF
pKW586	pGEX [GST-Gsp1Q71L]	4CD
pMW6	pGEX [GST-Gsp1]	4CD
pMW1	pTF155*Δ* C [GAL-His12-Blm10*Δ* C1804-2143]	4D
pMW2	pET21b [Blm10C aa1804-2143]	4D
pMW3	pGEX [GST-Blm10C aa 1749-2143]	4D
pMW4	pGEX [GST-Blm10C aa 1749-2143 W2021A]	4D
pGS467	pQE [6His-Gsp1]	4G
pNup53FL	pGEX [GST-Nup53]	4F

References:

pTF155 (Iwanczyk et al., 2006)

pMK210-4 (Hellmuth, K., D.M. Lau, F.R. Bischoff, M. Kuenzler, E.C. Hurt, and G. Simos. 1998. Yeast Los1p has properties of an exportin-like nucleocytoplasmic transport factor for tRNA. Mol. Cell. Biol. 18:6364-6386.)

pKW585 and pGS467 (Schlenstedt et al. 1995)

pNup53FL (Marelli et al. 1998)

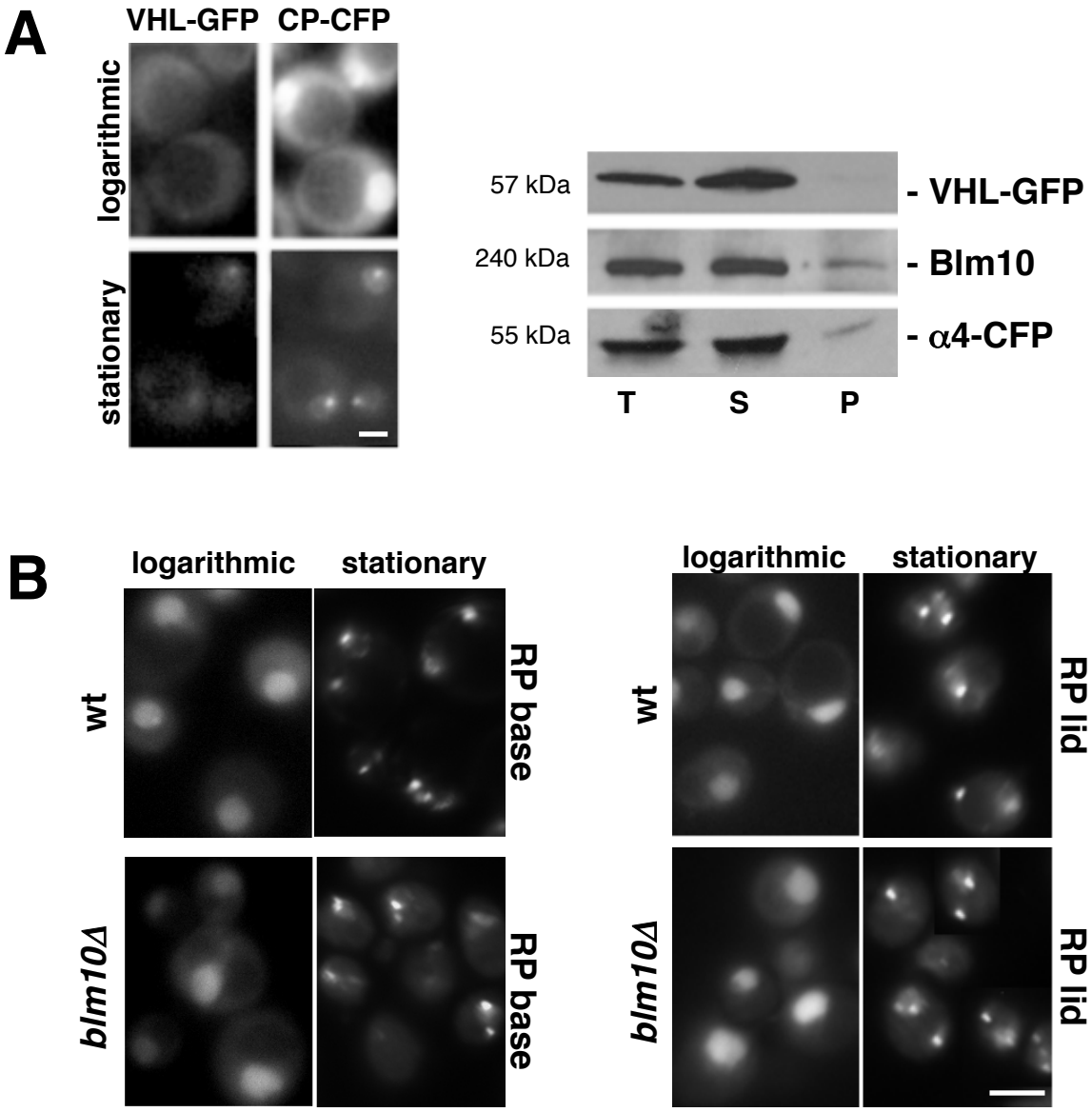
A
VHL-GFP
CP-CFP
logarithmic
stationary
57 kDa
240 kDa
55 kDa
- VHL-GFP
- Blm10
- α4-CFP
T
S
P
B
logarithmic
stationary
wt
blm10Δ
RP base
RP lid
C
logarithmic growth
stationary growth
wt
blm10Δ
Ump1-associated
precursor complexes

Figure S1

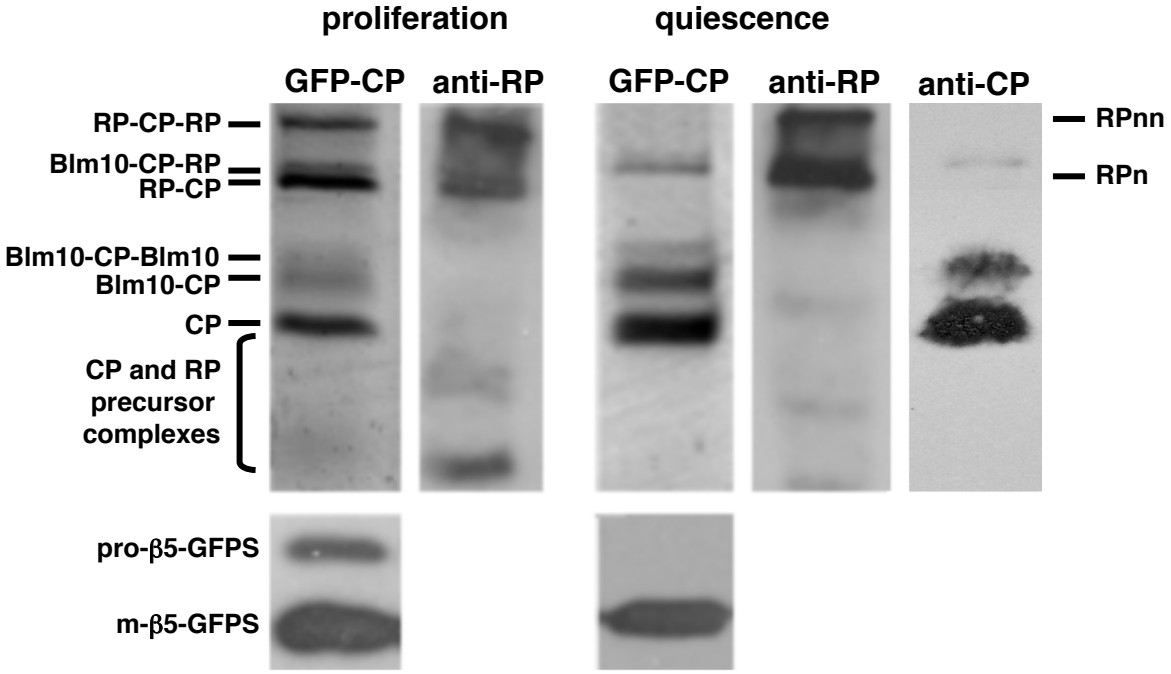
proliferation
quiescence
GFP-CP
anti-RP
GFP-CP
anti-RP
anti-CP
RP-CP-RP
Blm10-CP-RP
RP-CP
Blm10-CP-Blm10
Blm10-CP
CP
CP and RP precursor complexes
RPnn
RPn
pro-β5-GFPS
m-β5-GFPS

Figure S2

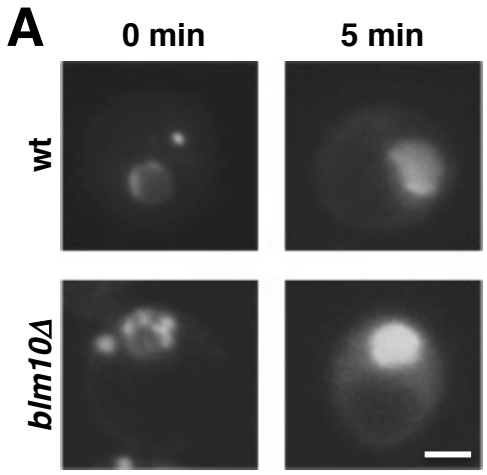
A
0 min
5 min
wt
blm10Δ

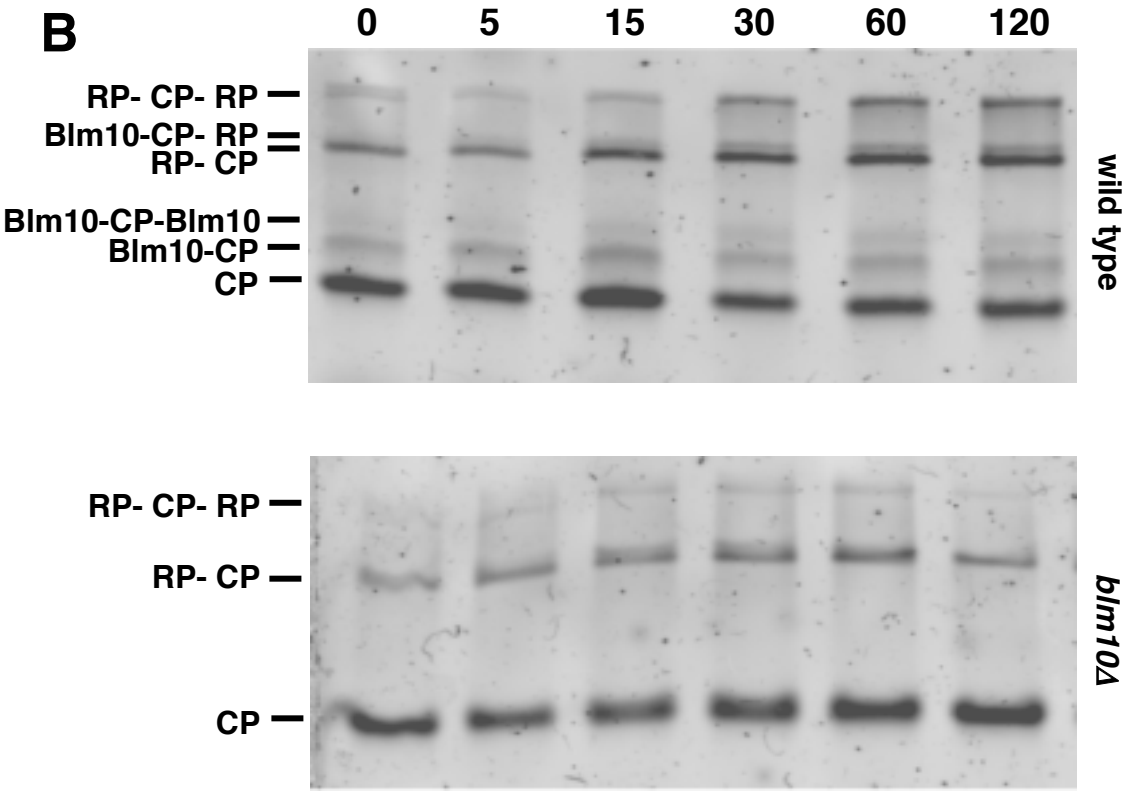
B
0
5
15
30
60
120
RP- CP- RP
Blm10-CP- RP
RP- CP
Blm10-CP-Blm10
Blm10-CP
CP
wild type
RP- CP- RP
RP- CP
CP
blm10Δ

Figure S3

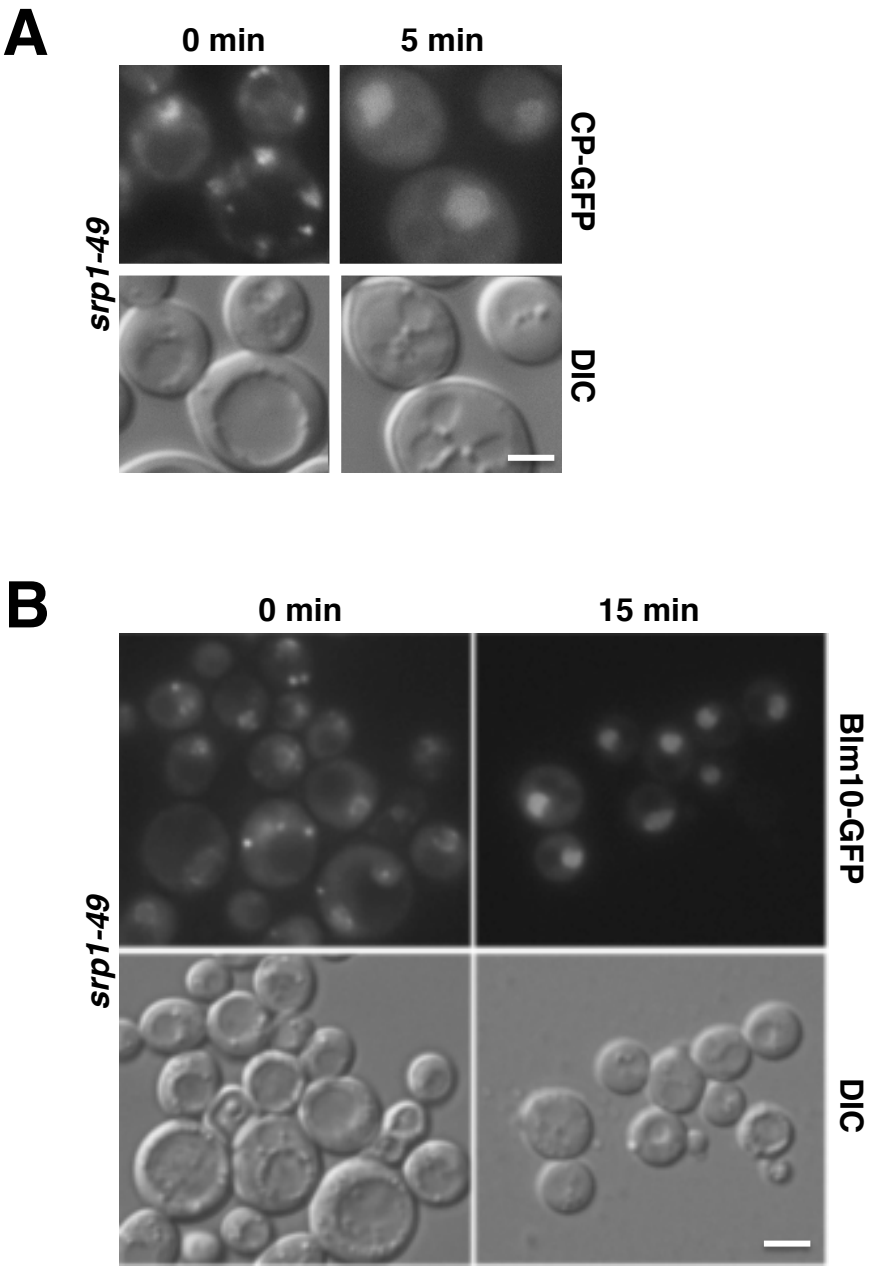
A
0 min
5 min
CP-GFP
srp1-49
DIC
B
0 min
15 min
Blm10-GFP
srp1-49
DIC

Figure S4

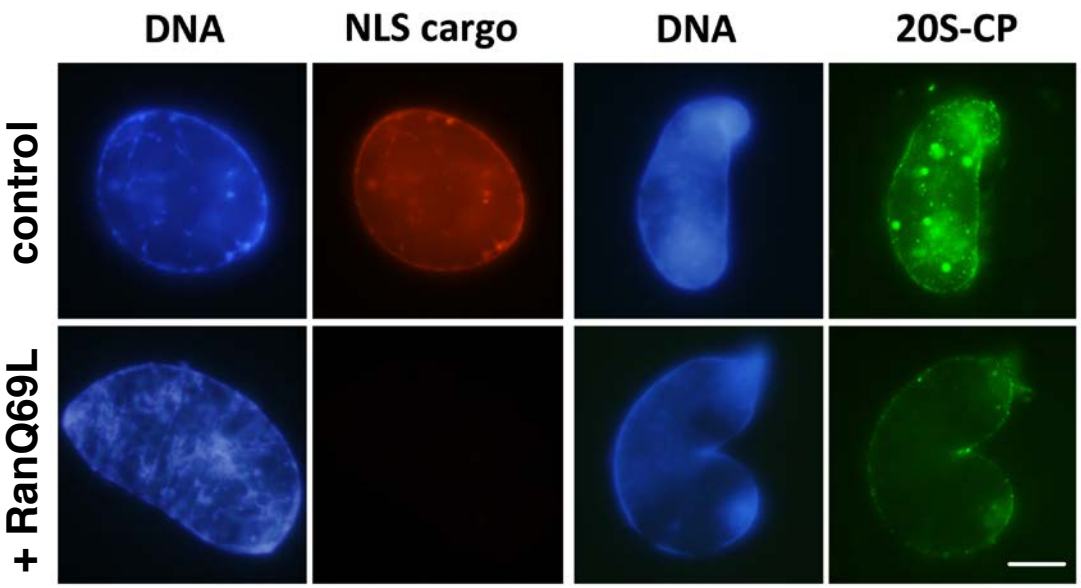
DNA
NLS cargo
DNA
20S-CP
control
+ RanQ69L

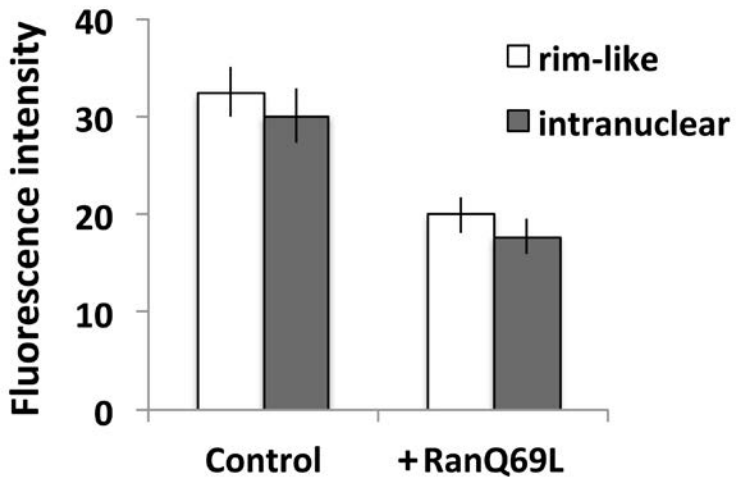
Fluorescence intensity
40
30
20
10
0
rim-like
intranuclear
Control
+RanQ69L

Figure S5

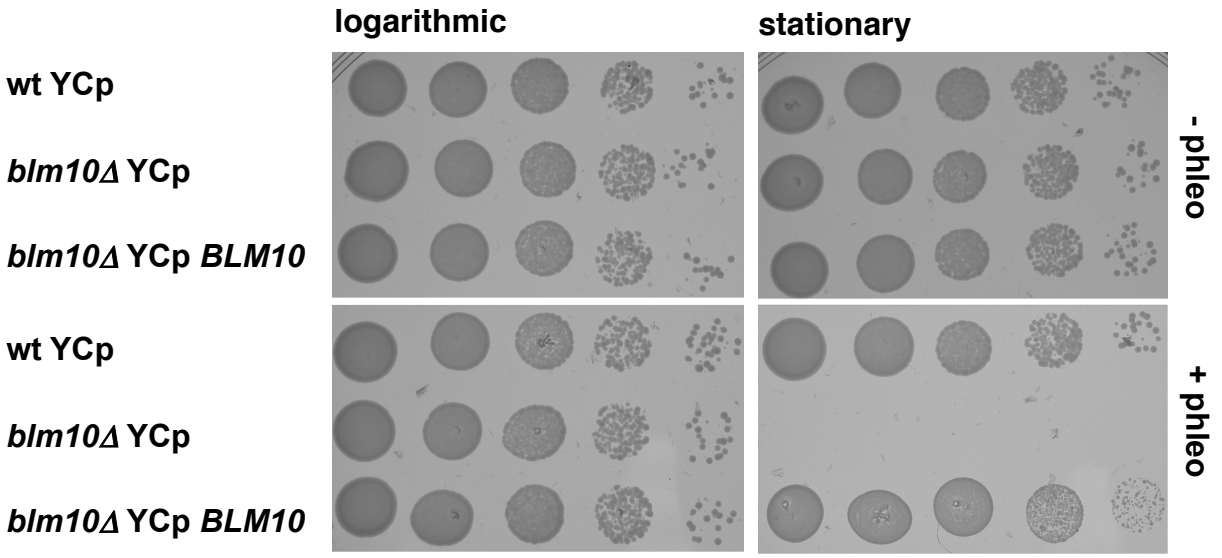
logarithmic
stationary
wt YCp
blm10Δ YCp
blm10Δ YCp BLM10
wt YCp
blm10Δ YCp
blm10Δ YCp BLM10
- phleo
+ phleo

Figure S6